Fall Detection and Personnel Tracking System Using Infrared Array Sensors

Zhixin Liu, *Member, IEEE*, Ming Yang, Yazhou Yuan, and Kit Yan Chan, *Member, IEEE*

***Abstract*—Body falling is a major risk of the older people. This paper proposes a non-contact scheme for detecting human body state using infrared array sensors, which has the advantages of low cost, easy implementation and high detection accuracy. For achieving real-time monitoring, rather than simple motion analysis, the system identifies suspicious points of body falling by simple positioning, which attempts to achieve the real-time implementation and reduces the analysis of irrelevant data. In addition, considering the influence of the radiation temperature result of the human body, the falling characteristics are included, and the clustering algorithm is proposed to tackle the problem of inaccurate determination of the area caused by the Otsu area detection. Then, a two-layer threshold system model is proposed for excluding jogging movements that are similar to the falling feature. Finally, the features are engaged with the random forest classifier in order to improve the classification rate. Experiments have shown that the proposed fall detection scheme is highly feasible and behaves good fall detection accuracy.**

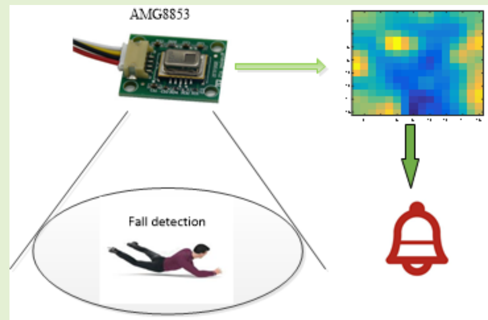

***Index Terms*—Fall detection, infrared array sensors, random forest classifier, detection accuracy.**

I. Introduction

IN THE next decades, human society is facing an ageing problem, and the proportion of the elderly population is increasing [1]. The health of the elderly has become the focus of attention. Falling is very harmful to the elderly and is considered as one of the most dangerous accidents for the elderly [2]. According to the data from Center for Disease Control and Prevention, more than one-third of the elderly fall every year, and accidental falls account for a large proportion [3]. In particular, the problem of falling down for an elderly person living alone may be life-threatening if an old man fell for a long time without assistance. Report shows that elderly people, who fell but can receive immediate help, can reduce the risk of death by 80% [4]. Therefore, it is necessary to design a set of intelligent fall detection systems for elderly people.

Manuscript received March 23, 2020; accepted April 12, 2020. Date of publication April 15, 2020; date of current version July 17, 2020. This work was supported in part by the National Natural Science Foundation of China under Grant 61873223 and Grant 61803328 and in part by the Natural Science Foundation of Hebei Province, China, under Grant F2019203095 and Grant F2017203084. The associate editor coordinating the review of this article and approving it for publication was Dr. Sanket Goel. *(Corresponding author: Zhixin Liu.)*

Zhixin Liu, Ming Yang, and Yazhou Yuan are with the Key Laboratory of Industrial Computer Control Engineering of Hebei Province, Yanshan University, Qinhuangdao 066004, China (e-mail: lzxauto@ysu.edu.cn).

Kit Yan Chan is with the Department of Electrical and Computer Engineering, Curtin University, Perth, WA 6102, Australia (e-mail: kit.chan@curtin.edu.au).

Digital Object Identifier 10.1109/JSEN.2020.2988070

In recent years, the fall detection system for elderly people has been continuously improved and has been applied to the daily life of elderly people living alone. For further analysis, it is necessary to propose accurate fall classification and detection techniques [5]. Wearable sensors are commonly used in fall detection systems. Inertial sensors such as accelerometers and gyroscopes are used to detect the movement status of the elderly [6]–[8]. After motion data is collected, appropriate thresholds are set to determine changes in the body during exercise. Since the smart phones are popular, traditional wearable devices are replaced with the smart phones to detect people falling [9]–[11]. In order to facilitate the wearing of the sensor and avoid affecting normal life, some researchers embed the sensors in the shoes. The experiment analyzes the tester's foot movement direction and the force condition to judge the tester's exercise state [12]. Although the wearable device can detect the fall state of the elderly, unfortunately, it requires the elderly to wear the equipment at all time.

In order to improve the detection accuracy and reduce the dependence of the detection equipment, digital cameras are generally used to capture the fall [13], [14]. Although the camera can capture the movement status of the elderly accurately and in real time, distinguishing the human body and the background from the video is still a challenging task. In addition, the camera is sensitive to light. If the detection environment changes brightly, the detection accuracy will be greatly reduced. Moreover, video detection violates the privacy of the person being tested, which is unacceptable for most

1558-1748 © 2020 IEEE. Personal use is permitted, but republication/redistribution requires IEEE permission.
See https://www.ieee.org/publications/rights/index.html for more information.

Authorized licensed use limited to: University of Adelaide. Downloaded on September 03,2021 at 01:18:45 UTC from IEEE Xplore. Restrictions apply.

people. In order to avoid this, depth cameras are generally used instead of traditional cameras [15]–[17], but large computation and high cost are still required.

In this paper, we discuss the problem of detecting human motion using infrared array sensors when actual heat source interference exists. We propose a device-free fall detection system leveraging the temperature of Infrared array sensor as the indicator. We define the area, which can be covered by infrared array sensor for fall detection, as the effective range area for performance evaluation. The infrared array sensor is used to detect various activities for a single person inside the effective area, and the developed detection scheme can achieve fall detection with high accuracy. The main contributions of this paper are summarized as follows:

(1) *Low cost and no invasion of privacy*. We exploit the feasibility of using temperature information of infrared array sensor for device-free fall detection. Compared with other fall detection systems, infrared array sensors can detect larger areas with fewer devices and lower cost. It is suitable for dark environment, and the monitoring is non-contact, while the detection system does not interfere personal privacy.

(2) *Low complexity and real time detection.* To implement the real-time fall detection system, we analyze the suspicious fall points by simple positioning. By analyzing suspicious points, real-time monitoring can be achieved while reducing the analysis of irrelevant data.

(3) *High detection accuracy*. A variety of improved extraction feature methods are proposed to improve the detection accuracy. For the case where the area of the Otsu detection area is inaccurate, a clustering algorithm is proposed. the double-layer threshold model is proposed to suppress interference caused by jogging, whose feature is similar to the fall. Also, we develop a random forest algorithm with better generalization ability to classify different human activities. Experimental results show that the system can achieve an average detection accuracy of 94%.

The rest of this paper is organized as follows. Section II reviews the related works, and the system structure and framework are given in Section III. In Section IV, we introduce the detailed design of fall detection system. Section V describes the experimental steps and algorithm introduction, followed by the evaluation results in Section VI. Finally, we give the conclusions and discussions of the future work in Section VII.

II. Related Works

Nowadays, many novel systems have been presented for fall detection. Since the infrared technology is more advanced, more and more attention has been paid on Passive Infrared(PIR) sensor based motion capturing for human detection. Infrared sensor-based human behavior detection not only avoids the intrusion of personal privacy caused by direct detection, but also has small size, low energy consumption and low cost. Kim *et al.* [18] developed the PIR sensor for collecting specific locations of residents. Multiple PIR sensors are installed on the wall for capturing location of the human body. Bayesian classifier is used to improve location accuracy. Although the PIR sensors can avoid personal privacy violations during detection, the sensor can only obtain location information of the human body and fail to obtain more behavior information, such as falling.

Furthermore, T. Liu and X. Guo adopted infrared sensors to detect human fall [19]. The infrared sensors are used to detect differences in the movement of different parts of the body and a distributed direction-sensitive infrared sensing approach is proposed for fall detection. In addition, a two-layer Markov model is introduced to identify fall events. However, the device can only detect the fall of a person in one direction, and the infrared sensor measurement angle will change with the test distance transformation. Therefore, the measurement accuracy is affected by the measurement distance greatly.

A person state detection method based on infrared array sensor is proposed in [20], where the temperature information obtained from the infrared array sensor is analyzed and classified into five fundamental states by support vector machine. However, this method ignores the influence of the detection angle. The method simply classifies the behavioral actions, and cannot detect the fall of the person in real time within the detection range.

Recently, more and more intelligent learning algorithms have been applied to fall detection systems [21]–[23]. Machine learning algorithms become the focus of research. However, machine learning algorithms have different effects in different environments and data sets. Some authors compare machine learning methods such as random forest, neural networks, regression trees, and support vector machines [24], [25]. Through the comparison, the random forest algorithm behaves higher stability and robustness with varying training parameters and better success rates and ROC analysis results.

In all, infrared sensor is very suitable for human motion detection. Analyzing the fall situation in real time is the focus of the current research. In this paper, we attempt to present a fall detection methodology supported by real-time detection. Through the improved method of extracting features, the most relevant features of the fall are obtained. The random forest algorithm is developed to improve the classification accuracy.

III. System Structure and Framework

Most fall detection systems operate in a similar manner, but the analysis of fall characteristics and other states alone are not sufficient for practical applications. Finding the fall feature in the dynamic is the key to the current fall detection technology. For real-time status detection, obtaining the location information of person is essential. The proposed system uses the personnel positioning to determine whether the current action has the possibility of falling, and analyzes the current action characteristics to obtain the final judgment. In order to be closer to the actual situation, the system first positions the personnel and then dynamically analyzes the fall action. When no fall action occurs, the sensor only performs positioning processing, and does not perform complex fall detection algorithm operations, which saves computation time.

The system fully considers the real-time and complexity of detection. In Fig. 1, the data collected by the sensor is

Authorized licensed use limited to: University of Adelaide. Downloaded on September 03,2021 at 01:18:45 UTC from IEEE Xplore. Restrictions apply.

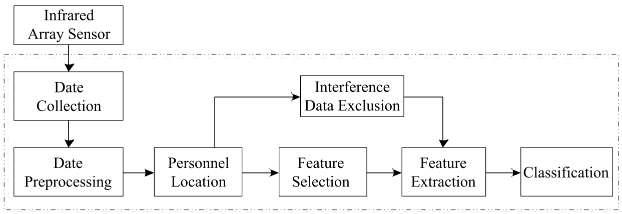

Fig. 1. Event-driven architecture for fall detection.

transferred to the PC host computer. First, to detect the state of the person from the low-resolution image, the data is pre-processed to remove the influence of the heat source and noise. Then, the detected person is positioned to determine whether there is a possibility of a fall at the detection time. For suspicious data of fall, the most obvious dynamic features of the fall are extracted. Finally, the machine learning algorithms are used to determine whether the current action is a fall.

IV. Detecting Falls Under Infrared Array Sensors

In this section, we discuss the algorithm for fall feature extraction in infrared array sensors. First, we use the infrared array sensor to find the location where the fall may occur. Then we introduce how the fall feature is selected and the feature extraction method is given. The last part introduces an improved method to improve the accuracy of the system.

A. Personnel Positioning and Stationary Point Acquisition

Due to the influence of heat source and background temperature, people's characteristic information cannot be obtained simply from the original data. In order to eliminate the influence of heat sources and background temperature on personnel detection, we use bicubic interpolation and background subtraction to separate foreground and background and obtain human information. Figure 2 shows the acquisition data processing. Firstly, it collects the background temperature and performs interpolation [26] on the data frame. The current frame uses background subtraction to remove the other heat and background temperature. To facilitate the extraction of fall features, the interpolated data is scaled to the original image size.

In reality, since we do not know when and where people will fall, we cannot make a qualitative analysis of an action. Therefore, the falling location is first determined and then the falling action is analyzed. Through a lot of experiments, it is found that the elderly will stay still for a short time or longer time after falling. This is a sign of unconsciousness, but it provides an incentive to detect whether the elderly fall. According to the sensor response time, to reduce resource consumption, sampling is performed every four frames. As shown in figure 3, binarization is first performed on the above data. Second, we use the connected component method to select the largest area block and identify its centroid position. The asterisk graphic in the figure indicates the target position.

When the centroid coordinates appear 5 or more times during the sampling process, the person is considered to be

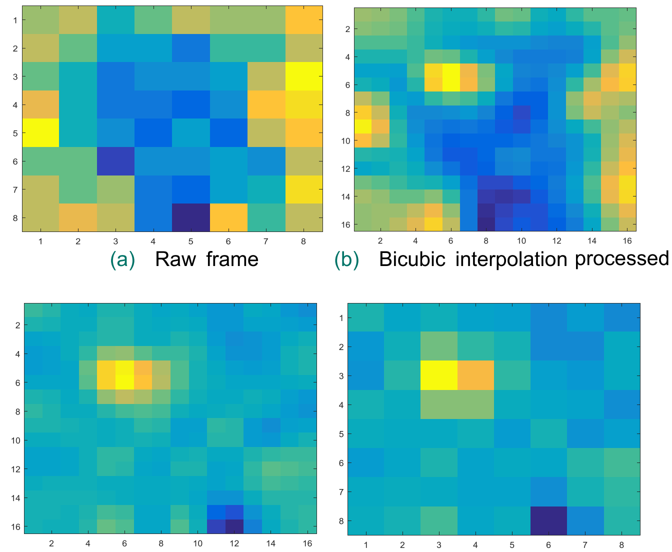

(a) Raw frame (b) Bicubic interpolation processed

(c) Background subtraction frame (d) Restore original frame

Fig. 2. The Initial data processing.

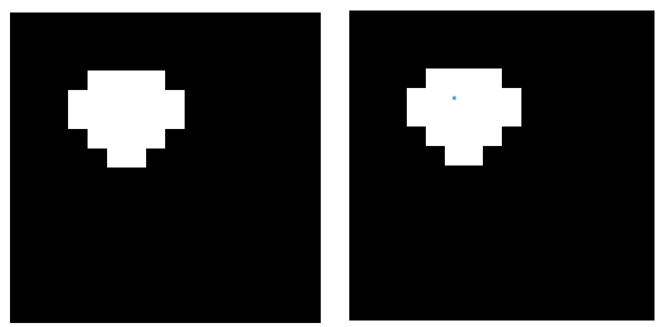

(a) Binarized image (b) Centroid position image

Fig. 3. Target location.

stationary. Excluding the influence of the detection error, if the detection coordinates are adjacent to the pixel at the positioning position, it is also considered to be the same detection position. The stationary point is the suspicious fall point which may occur during the detection process.

$$T_{sta} = \begin{cases} 0 & n < 5 \\ 1 & n \geq \end{cases} \tag{1}$$

where T_{sta} is the threshold value in the detection system for distinguishing whether the person is still in figure 2.

B. Fall Feature Extraction

The state of motion of the person is not fixed. There are many manifestations from mobile state to stationary state. The characteristics from the motion to the static are the key issues. We only focus on the results of the movement. For example, although the fall is a continuous movement, the final state is static. Therefore, the state of motion is only jogging and walking. The transformation relationship of various states is shown in figure 4.

Since the fall state will only appear before and after the quiescent state, we extract the most suitable features for

Authorized licensed use limited to: University of Adelaide. Downloaded on September 03,2021 at 01:18:45 UTC from IEEE Xplore. Restrictions apply.

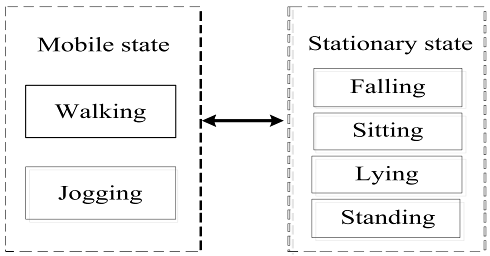

Fig. 4. Motion state transition diagram.

detecting falls by experimental data. The selected features are given as follows.

a) Stationary arrival time T_{re}: The sensor information is the temperature measurement for each pixel. When a person is within the detection area, the temperature of the sensor changes, and also the temperature change trend of different action is different. When the human body is stationary at a certain pixel position, the temperature at that position rises from the ambient temperature to the body temperature. Different operating temperatures vary from ambient temperature to body temperature, which is an important feature for judging whether the person falls or not.

$$T_{re} = T_{bg} - T_{st} \tag{2}$$

where T_{bg} is the background temperature before the sudden change in temperature, and T_{st} is the temperature at which the person is detected after the sudden change.

b) Static detection area S_r: When the person enters the detection range, the sensor can monitor the pixel size of each state. The detection area of the upright state and the lying down state is very different. Therefore we adopt this important feature to distinguish between falls and other states.

First, we obtain an 8*8 infrared array temperature matrix through data preprocessing. Note that the method is also suitable to other pixels, such as 16*4, 32*24. It just needs to change the dimension of temperature matrix.

$$T = \begin{bmatrix} T_{11} & T_{12} & \cdots & T_{18} \\ T_{21} & T_{22} & \cdots & T_{28} \\ \cdots & \cdots & \ddots & \cdots \\ T_{81} & T_{82} & \cdots & T_{88} \end{bmatrix} \tag{3}$$

where $T_{i,j}$ is temperature value of one of the 64 pixels. In order to achieve automatic detection of the area, we adopt the Otsu method [27]. We use the global adaptive threshold obtained by the Otsu method to distinguish whether the pixel is the detection area.

$$S_r = \begin{cases} 1 & T_{ij} \geq t_{gl} \\ 0 & T_{ij} < t_{gl} \end{cases} \tag{4}$$

where t_{gl} is the global adaptive threshold of the Otsu method. When the pixel temperature is greater than the threshold, the area is recorded as 1, otherwise it is 0. The threshold is given as

$$t_{gl} = \max\left[w_0(t) \times (u_0(t) - u)^2 + w_1 \times (u_1 - u)^2\right] \tag{5}$$

$w_0(t)$is the background ratio, $u_0(t)$ is the background mean, $w_1$is the foreground ratio, $u_1(t)$ is the foreground mean, and u is the mean of the entire image.

c) Detection area of the law S_s: It refers to the statistical rule of the area of two pixels before static and the area of pixels at static. The previous section shows that the detection process is dynamic. Falling is not an instant action and detecting a fall may require multiple frames. The temperature of the affected pixel position changes in the duration of the action.

$$S_s = S_p + S_r \tag{6}$$

where S_p is the detection area of the pixel before the person is still; S_r is the area of the above-mentioned detection at rest. Among them, the area detection method is same as above

However, considering the actual detection environment, the area detected by the Otsu method is not necessarily accurate. The human body is radiated. Simply dividing the temperature into the environment and the human body may cause errors, and the system may make wrong classification for fall detection. In addition, some actions similar to falls may also have an impact on the classification. It is necessary to develop a simple and reasonable method for fall detection.

C. Improved Detection Method

1) Improved Area Detection Method: Considering that the human body has a radiation temperature in actual detection, a method for detecting temperature area by clustering method is proposed. This method is mainly for area detection when standing upright. The detection temperature is mainly concentrated near the head when standing upright. Therefore, there is a large temperature radiation, while the temperature radiation of other body parts is small. Moreover, when the human body is upright, the sensing distance is close and the detection temperature is large. The radiation temperature is more obvious. Therefore, using the clustering method to detect the temperature region can effectively eliminate the interference. Although the fall area farther from the sensor also generates radiation, most of the area detected by the clustering method is the body temperature, which has little effect on the result.

This experiment uses the clustering method [28] to divide the detection temperature into three layers: background temperature, human body radiation temperature and human body temperature. As illustrated in Section 4, Infrared array sensor has 8*8 pixels and can collect 64 frames of temperature information. We use the temperature information of 64 sensor outputs, $\mathbf{x} = [x_1, x_2, \cdots, x_{64}]$, as the input of the clustering algorithm and the result is divided into three clusters, $\mathbf{c} = [c_1, c_2, c_3]$. We optimize the classification results by minimizing the square error.

$$E = \sum_{i=1}^{k} \sum_{x \in c_i} \|\mathbf{x} - \mathbf{u}_i\|_2^2 \tag{7}$$

where $\mathbf{u}_i = \frac{1}{\|u_i\|} \sum_{x \in c_i} \mathbf{x}$ is the mean vector of the cluster c_i In this experiment, k is set as 3.

Authorized licensed use limited to: University of Adelaide. Downloaded on September 03,2021 at 01:18:45 UTC from IEEE Xplore. Restrictions apply.

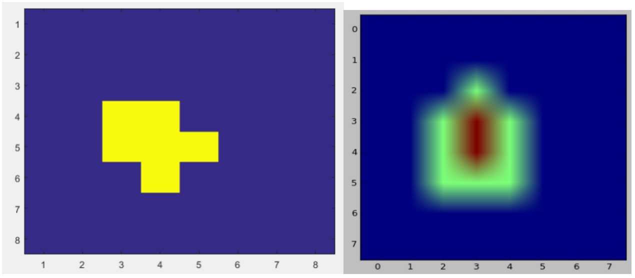

(a) Number of pixel areas of Otsu (b) Number of pixel areas of Clustering method

	0	1	2	3	4	5	6	7
0	0	0	0	0	0	0	0	0
1	0	0	0	0	0	0	0	0
2	0	0	0	1	0	0	0	0
3	0	0	1	2	1	0	0	0
4	0	0	1	2	1	0	0	0
5	0	0	1	1	1	0	0	0
6	0	0	0	0	0	0	0	0
7	0	0	0	0	0	0	0	0

(c) Clustering algorithm three types of distribution labels

Fig. 5. Comparison of two area detection methods.

Clustering divides the temperature into three categories. Because the clustering label is automatically marked, the one with the highest temperature is the human body label, and the lowest temperature is the background label. As shown in figure 5, the number of pixel areas detected by the Otsu method is 6. The improved clustering algorithm detects 2 pixel areas. In contrast, the size of the pixel area detected by the clustering method is more in line with the actual situation.

2) Jogging Data Exclusion: Through a lot of experiments, we found that, among the above extracted features, the characteristics of jogging and falling are relatively similar. If two types of actions are indistinguishable, it leads to the wrong classification, which will affect the classification accuracy. Since the fall process does not complete in an instant, the fall will last a few pixels before stopping. Therefore, we extract the corresponding features by the time difference before the static, and obtain a more accurate detection rate. Moreover, jogging and falling have obvious differences in other features, which provide an effective way to eliminate jogging.

Through experimental analysis, several features are extracted as follows.

a) Kurtosis[29]: The kurtosis of the temperature detected by one pixel before static is defined as.

$$excess_k = \frac{E\,(x-u)^4}{\sigma^4} - 3 \tag{8}$$

Kurtosis is the standard fourth-order center distance for distribution.

b) Peak distance P_d: It represents the distance between two peaks. This feature reflects the time taken from one pixel area to another during the motion.

c) Detection area of the pixel before the static T_{bg}: When the jogging speed is too fast, detection area is excessive during data processing. This is not easy to distinguish that the motion is jogging or falling. Therefore, it is necessary to distinguish jogging and remove it to avoid false alarm.

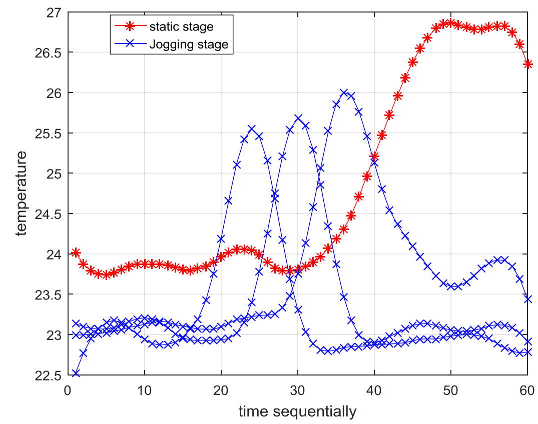

Fig. 6. Temperature change during jogging.

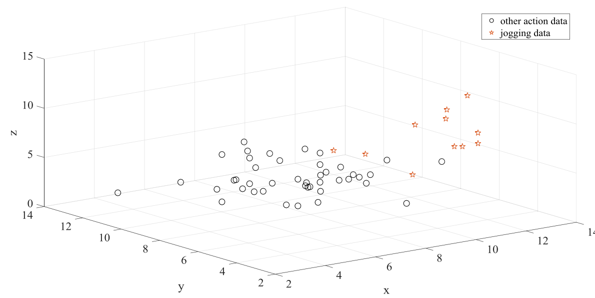

Fig. 7. The magnitude distribution of original features.

The characteristics are quite obvious during jogging. During the jogging, the kurtosis is large, and the peak distance is small. The stationary time is short since the motion is fast.

Thus, a three-dimensional map of features is introduced. As shown in figure 7, the difference between jogging and other actions is more obvious. General classifiers can get better classification results. This can distinguish between jogging and other actions, even if the individual data classification is wrong, it will not have much impact on the training. At the same time, if there are fewer training features, the experimental results will be contingent. Experimental results show that the temperature will be stratified during the fall. During a fall, the same pixel will detect different positions of falling body, so the detection temperature will also be different. However, due to the heat radiation of the human body, the temperature of the surrounding detection pixels will also rise, and stratification will occur as shown in figure 8. Therefore, the stratification phenomenon cannot be regarded as a distinct feature. However, the human body radiation temperature and the fall detection temperature are not the same. The numerical features can be used to distinguish whether the detection process falls or not.

d) Stratified temperature difference T_d and peak temperature difference T_p: Using the phenomenon of stratification, two temperature quantities can be obtained.

$$\begin{aligned} T_p &= T_{pt} - T_{st} \\ T_d &= T_{st} - T_{bs} \end{aligned} \tag{9}$$

Authorized licensed use limited to: University of Adelaide. Downloaded on September 03,2021 at 01:18:45 UTC from IEEE Xplore. Restrictions apply.

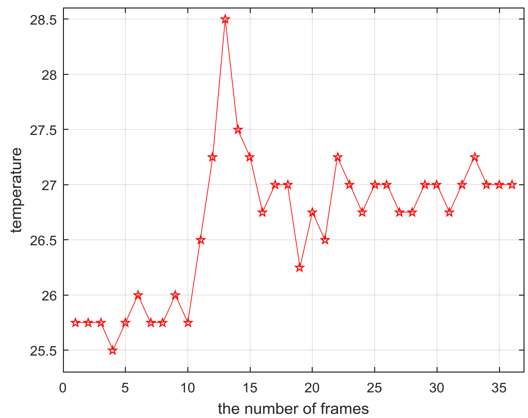

Fig. 8. Temperature stratification.

where T_{pt} is peak temperature after stratification; T_{st} is average temperature after stratification; T_{bs} is average temperature before stratification.

V. Experimental Studies

A. Experimental Setup

To test the performance of the proposed system, we set up a test system. As shown in figure 9, the experimental site is a laboratory and the sensors are placed on the ceiling. The used sensor is the AMG8853 infrared array sensor made by Panasonic of Japan. The fall detection algorithm is executed on a PC. It runs under the Windows operating system. The temperature data is collected by the infrared array sensor and transmitted through the USB to the host computer.

In the experiments, a total of 8 experimental subjects were selected. To avoid the influence of height on the experiment, 7 males and 1 female were selected. All volunteers are between 160cm and 180cm tall. In the coverage of the infrared array sensor, different experimental subjects perform walking, jogging, squatting, lying down, falling, still, etc. The effective detection distance of this sensor is 5 meters. The sensor is 3.5m above the ground and can detect space of about 4m×4m. The lab has different heat sources and complex environments.

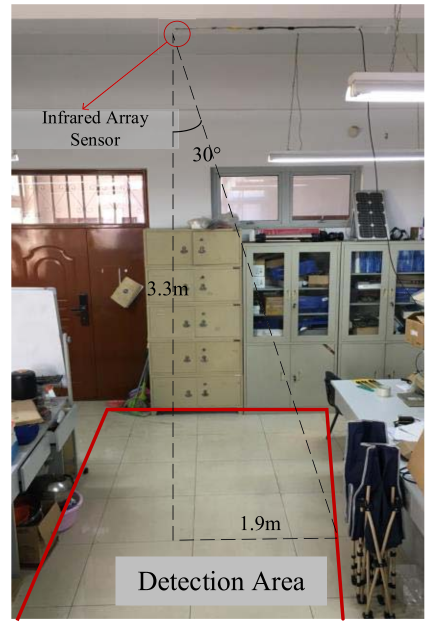

Fig. 9. Experimental environments.

Algorithm 1 Random Forest Algorithm

Step1: For given training samples, new sample $(x_{1j}, y_1), \cdots, (x_{ij}, y_i)$ can be built based on the original data set$(x_{1n}, y_1), \cdots, (x_{mn}, y_m)$ through sampling randomly and repeatedly i times.

Step 2: Building a decision tree based on randomly selected sample.

Step 3: Repeat Step1-2, we can get strong learners through a variety of weak learners.

Step 4: For a given set of testing samples $\left(x'_{1j}, x'_{2j}, \cdots, x'_{ij}\right)$, let all trees vote to the input vector x'_{ij}.

Step 5: Count all votes to find the highest vote which is the label y'_i of the vector.

Step 6: The final result is determined by the correct voting ratio and is verified by unselected off-bank data.

B. Random Forest Classification

The machine learning algorithm is used to train and classify the data, and a historical database is established. To improve the generalization ability of the classifier, the random forest (RF) classifier is introduced, which has strong anti-interference ability, fast training speed and can perform unbalanced classification. The RF algorithm is an integrated learning algorithm that is essentially a combination of multiple decision trees [30]. All selected trees in RF are independently and identically distributed, and each tree is randomly selected. Random forests use two random characteristics and select the most popular categories of trees by voting in order to improve detection rates of weak learners. The random variables are often introduced to control the growth of each tree. The whole process is summarized in Algorithm 1.

Figure 10 gives the flowchart of the fall detection system. First, we preprocess the data collected by the infrared array sensor. With differential temperature information, we can locate the general position of the tested person and find the suspected fall point. Then, two layers of threshold detection is set up to improve system detection accuracy. The first threshold is to exclude the impact of jogging data on classification results. It is able to distinguish between falls and other states after excluding jogging data. The second one is to ultimately distinguishes between falls and other states. We use the randomized forest algorithm to classify different motions, and set accuracy threshold to improve the classification accuracy.

$$Fall = \begin{cases} 1 & \text{If training accuracy } 1 < Thereshold\ 1 \text{ and} \\ & \text{training accuracy } 2 > Threshlod\ 2 \\ 0 & \text{Otherwise} \end{cases}$$

where *Threshold*1 is defined in the first-layer classifier in order to exclude the impact of the jogging data, and *Threshold*2 is

Authorized licensed use limited to: University of Adelaide. Downloaded on September 03,2021 at 01:18:45 UTC from IEEE Xplore. Restrictions apply.

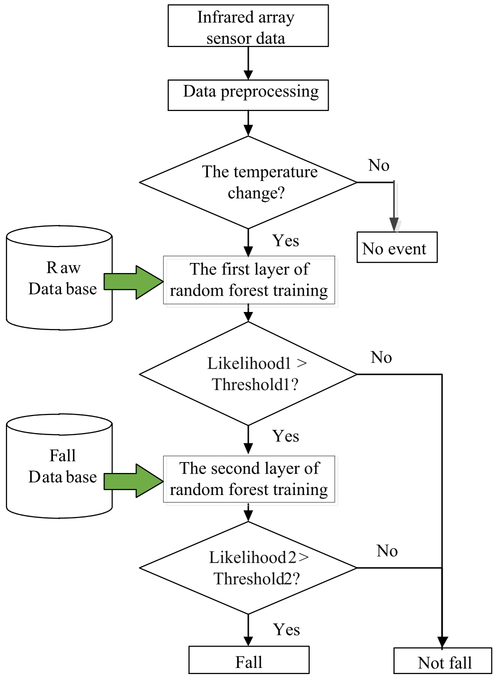

Fig. 10. The flowchart of the fall detection system.

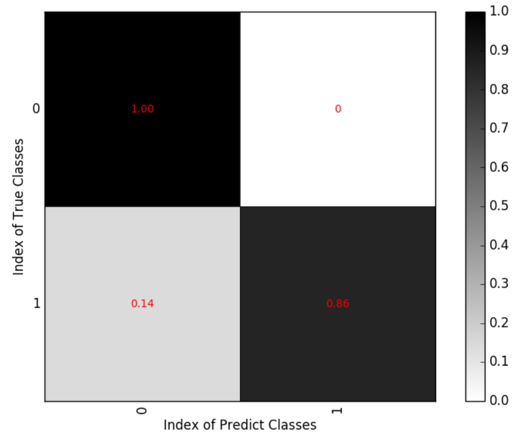

Fig. 11. Confusion matrix.

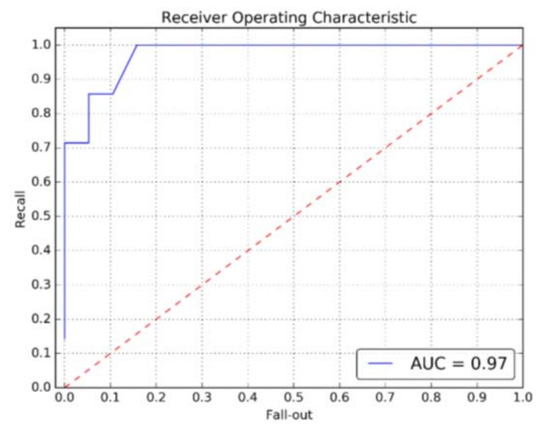

Fig. 12. ROC curve for the classification system.

defined in the second-layer random forest in order to detect the fall. All thresholds are set according to the actual situation.

VI. Experimental Results

In order to evaluate the system performance, we use the accuracy rate as an indicator of training performance to distinguish between falls and other motion states. However, for a two-category problem, it is not enough to analyze the accuracy alone. In addition to the accuracy rate, we also take into account the classification precision and recall rate. So the confusion matrix is proposed to evaluate the performance of the classification system. The rows of the confusion matrix represent the prediction classification, and the columns represent the actual classification. Based on the real and predicted values, we can compute the recall and precision of the classifier. In addition to the criteria for judging the overall classification model, such as the accuracy, the confusion matrix can analyze the characteristics of each class to make the system more intuitive. After performing the normalization, all the values can be successfully normalized in the range [0, 1] as shown in figure 11. The diagonal value of the matrix is higher and the overall performance of the system is better.

To evaluate the performance of the classifier, a receiver operating characteristic (ROC) curve and relevant analysis for the classification system is also presented. The classifier performance is indicated by the ROC curve which illustrates the false positive rate (FPR) and true positive rate (TPR) for each category. When the ROC curve is closer to the upper left corner of the image, the higher the accuracy is achieved. Figure 12 shows the ROC curve and AUC value.

Table I shows the various indicators of the system. The evaluation results show performance from three aspects: precision, recall rate and f1 score. Through the different indicator, especially the analysis of the fall event, the feasibility of the scheme is validated.

TABLE I
Training Performance Indicator

parameters	precision	recall	f1-score
Normal event	0.95	1.0	0.97
Fall event	1.0	0.86	0.92
Average/total	0.96	0.96	0.96

Among parameters in random forest, the number of the trees has the greatest influence on the final result. The model accuracy is improved with the optimal parameter. In general, when the number of trees increases, the system accuracy also increases. However, too many trees will not only affect the efficiency of operation, but also cause unnecessary over-fitting effects. Furthermore, the obtained results, using the training set and the test set, are in the case of a fixed parameter random state. Therefore, in order to eliminate the contingency, we select the average result after ten times of random state, which greatly eliminates the contingency of detection and improves the reliability of the system. As seen in figure 13, with the increasing number of trees, the system accuracy will be improved. When the system accuracy has reached a certain accuracy, the improvement of training results saturates.

Authorized licensed use limited to: University of Adelaide. Downloaded on September 03,2021 at 01:18:45 UTC from IEEE Xplore. Restrictions apply.

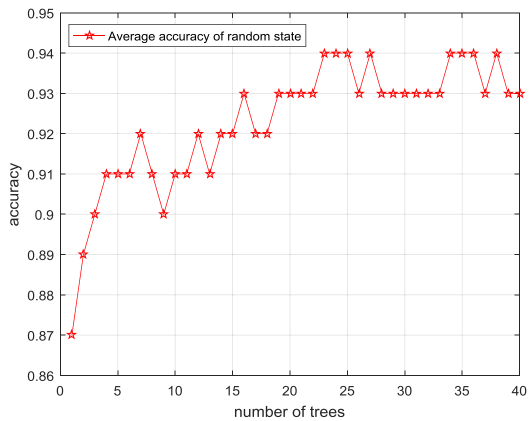

Fig. 13. Average accuracy of random states under different trees.

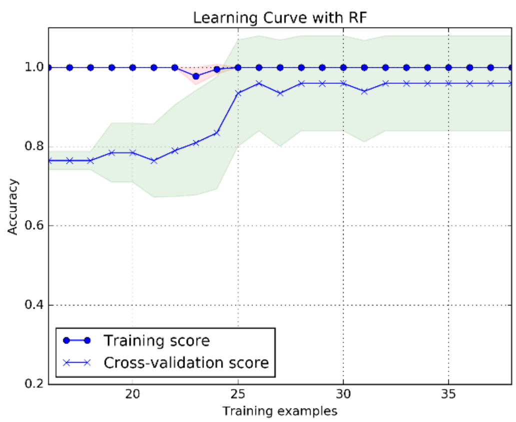

Fig. 14. Learning curve with RF.

TABLE II
TRAINING PERFORMANCE INDICATOR

parameters	Without extra processing	With area improvement processing	Final test result
precision(%)	83.33	90.83	94
AUC value	0.77	0.88	0.97

Therefore, when the number of tree selected by the system is 23, the system shows the best state. The results show that the average accuracy reaches 94% and the highest can reach 96%.

Besides, the number of the training samples is another important parameter, which, in general, directly affects the accuracy of the classifier and the stability of the model. However, in practical training, too many training samples may not improve system performance. Thus, a suitable training samples can reduce the complexity of the system and improve system performance. Learning curve indicates the benefit of adding more training data and whether the estimator is suffered more from a variance error or a bias error. The variance and deviation of different training sets are different. If both the training score and verification score do not increase as the size of the training set increases, it is not necessary to increase the training set. As shown in figure 14, when the number of training samples is 32, the maximum accuracy of 94% can be obtained.

Table II shows the results of the various indicators for the three test phases. The relevant algorithms in the experimental studies run on an Intel i5-3230M CPU 2.6GHz computer by Python and Matlab. The results show that the accuracy of the experimental improvement method is 94%, and the AUC value also increased from the original value of 0.77 to 0.97.

VII. CONCLUSIONS

In order to ensure the privacy of the user and improve accuracy and generalized ability of fall detection system, a novel scheme based on infrared array sensor is proposed in the paper. This scheme achieves two main advantages. First, the proposed system uses temperature analysis and simple personnel positioning, in order to detect suspicious points of fall. Analyzing the suspected points not only detects the fall state in real time, but also reduces the analysis of irrelevant data. Second, the layered processing of data and the enhanced methods in the feature extraction process improve the accuracy. To achieve better generalization ability and more accurate classification, random forest classifier is adopted. The results show that the performance of the system is stable and reliable. The high detection accuracy is achieved. To be more practical, a larger detection range is required. In future work, multiple sensors should be applied to fall detection to extend coverage.

REFERENCES

[1] United Nations, New York, NY, USA. (2015). *World Population Ageing*. [Online]. Available: http://www.un.org/en/development/desa/population/publications/pdf/ageing/WPA2015_Report.pdf
[2] J. A. Stevens, "Falls among older adults—Risk factors and prevention strategies," *J. Saf. Res.*, vol. 36, no. 4, pp. 409–411, Jan. 2005.
[3] Y. Wang, K. Wu, and L. M. Ni, "WiFall: Device-free fall detection by wireless networks," *IEEE Trans. Mobile Comput.*, vol. 16, no. 2, pp. 581–594, Feb. 2017.
[4] N. Noury, P. Rumeau, A. K. Bourke, G. Ólaighin, and J. E. Lundy, "A proposal for the classification and evaluation of fall detectors," *IRBM*, vol. 29, no. 6, pp. 340–349, Dec. 2008.
[5] K. Chaccour, R. Darazi, A. H. El Hassani, and E. Andres, "From fall detection to fall prevention: A generic classification of fall-related systems," *IEEE Sensors J.*, vol. 17, no. 3, pp. 812–822, Feb. 2017.
[6] F. Bianchi, S. J. Redmond, M. R. Narayanan, S. Cerutti, and N. H. Lovell, "Barometric pressure and triaxial accelerometry-based falls event detection," *IEEE Trans. Neural Syst. Rehabil. Eng.*, vol. 18, no. 6, pp. 619–627, Dec. 2010.
[7] J. K. Lee, S. N. Robinovitch, and E. J. Park, "Inertial sensing-based pre-impact detection of falls involving near-fall scenarios," *IEEE Trans. Neural Syst. Rehabil. Eng.*, vol. 23, no. 2, pp. 258–266, Mar. 2015.
[8] P. Pierleoni, A. Belli, L. Palma, M. Pellegrini, L. Pernini, and S. Valenti, "A high reliability wearable device for elderly fall detection," *IEEE Sensors J.*, vol. 15, no. 8, pp. 4544–4553, Aug. 2015.
[9] L.-J. Kau and C.-S. Chen, "A smart phone-based pocket fall accident detection, positioning, and rescue system," *IEEE J. Biomed. Health Informat.*, vol. 19, no. 1, pp. 44–56, Jan. 2015.
[10] Z. Liu, L. Gao, Y. Liu, X. Guan, K. Ma, and Y. Wang, "Efficient QoS support for robust resource allocation in blockchain-based femtocell networks," *IEEE Trans. Ind. Informat.*, early access, Sep. 3, 2019, doi: 10.1109/TII.2019.2939146.
[11] Y.-W. Bai, S.-C. Wu, and C.-L. Tsai, "Design and implementation of a fall monitor system by using a 3-axis accelerometer in a smart phone," *IEEE Trans. Consum. Electron.*, vol. 58, no. 4, pp. 1269–1275, Nov. 2012.
[12] L. Montanini, A. Del Campo, D. Perla, S. Spinsante, and E. Gambi, "A footwear-based methodology for fall detection," *IEEE Sensors J.*, vol. 18, no. 3, pp. 1233–1242, Feb. 2018.
[13] H. Foroughi, B. S. Aski, and H. Pourreza, "Intelligent video surveillance for monitoring fall detection of elderly in home environments," in *Proc. 11th Int. Conf. Comput. Inf. Technol.*, Dec. 2008, pp. 219–224.

Authorized licensed use limited to: University of Adelaide. Downloaded on September 03,2021 at 01:18:45 UTC from IEEE Xplore. Restrictions apply.

[14] H. Foroughi, H. S. Yazdi, H. Pourreza, and M. Javidi, "An eigenspace-based approach for human fall detection using integrated time motion image and multi-class support vector machine," in *Proc. Int. Conf. Signal Process.*, 2008, pp. 1499–1503.

[15] E. E. Stone and M. Skubic, "Fall detection in homes of older adults using the microsoft kinect," *IEEE J. Biomed. Health Informat.*, vol. 19, no. 1, pp. 290–301, Jan. 2015.

[16] Z.-P. Bian, J. Hou, L.-P. Chau, and N. Magnenat-Thalmann, "Fall detection based on body part tracking using a depth camera," *IEEE J. Biomed. Health Informat.*, vol. 19, no. 2, pp. 430–439, Mar. 2015.

[17] K. I. Withanage, I. Lee, R. Brinkworth, S. Mackintosh, and D. Thewlis, "Fall recovery subactivity recognition with RGB-D cameras," *IEEE Trans. Ind. Informat.*, vol. 12, no. 6, pp. 2312–2320, Dec. 2016.

[18] H. H. Kim, K. N. Ha, S. Lee, and K. C. Lee, "Resident location-recognition algorithm using a Bayesian classifier in the PIR sensor-based indoor location-aware system," *IEEE Trans. Syst., Man, Cybern. C, Appl. Rev.*, vol. 39, no. 2, pp. 240–245, Mar. 2009.

[19] T. Liu, X. Guo, and G. Wang, "Elderly-falling detection using distributed direction-sensitive pyroelectric infrared sensor arrays," *Multidimensional Syst. Signal Process.*, vol. 23, no. 4, pp. 451–467, Dec. 2012.

[20] S. Mashiyama, J. Hong, and T. Ohtsuki, "Activity recognition using low resolution infrared array sensor," in *Proc. IEEE Int. Conf. Commun. (ICC)*, Jun. 2015, pp. 495–500.

[21] S. Yu, H. Chen, and R. A. Brown, "Hidden Markov model-based fall detection with motion sensor orientation calibration: A case for real-life home monitoring," *IEEE J. Biomed. Health Informat.*, vol. 22, no. 6, pp. 1847–1853, Nov. 2018.

[22] Y. Yuan, X. Li, Z. Liu, and X. Guan, "Occupancy estimation in buildings based on infrared array sensors detection," *IEEE Sensors J.*, vol. 20, no. 2, pp. 1043–1053, Jan. 2020.

[23] W. Min, H. Cui, H. Rao, Z. Li, and L. Yao, "Detection of human falls on furniture using scene analysis based on deep learning and activity characteristics," *IEEE Access*, vol. 6, pp. 9324–9335, 2018.

[24] V. Rodriguez-Galiano, M. Sanchez-Castillo, M. Chica-Olmo, and M. Chica-Rivas, "Machine learning predictive models for mineral prospectivity: An evaluation of neural networks, random forest, regression trees and support vector machines," *Ore Geol. Rev.*, vol. 71, pp. 804–818, Dec. 2015.

[25] X. Yu, "Approaches and principles of fall detection for elderly and patient," in *Proc. 10th Int. Conf. e-Health Netw., Appl. Services (HealthCom)*, Jul. 2008, pp. 42–47.

[26] I. Ashraf, S. Hur, and Y. Park, "An investigation of interpolation techniques to generate 2D intensity image from LiDAR data," *IEEE Access*, vol. 5, pp. 8250–8260, 2017.

[27] J. Xue and D. Titterington, "t-tests, F-tests and Otsu's methods for image thresholding," *IEEE Trans. Image Process.*, vol. 20, no. 8, pp. 2392–2398, Aug. 2011.

[28] H. Frigui and R. Krishnapuram, "A robust competitive clustering algorithm with applications in computer vision," *IEEE Trans. Pattern Anal. Mach. Intell.*, vol. 21, no. 5, pp. 450–465, May 1999.

[29] Z. Xu and P. Liu, "Blind multiuser detection by kurtosis maximization/minimization," *IEEE Signal Process. Lett.*, vol. 11, no. 1, pp. 1–4, Jan. 2004.

[30] L. Calderoni, M. Ferrara, A. Franco, and D. Maio, "Indoor localization in a hospital environment using random forest classifiers," *Expert Syst. Appl.*, vol. 42, no. 1, pp. 125–134, Jan. 2015.

Zhixin Liu (Member, IEEE) received the B.S., M.S., and Ph.D. degrees in control theory and engineering from Yanshan University, Qinhuangdao, China, in 2000, 2003, and 2006, respectively. He is currently a Professor with the Institute of Electrical Engineering, Yanshan University. His current research interests include performance optimization and energy efficient protocol design in wireless sensor networks.

Ming Yang is currently pursuing the M.S. degree in control science and engineering with Yanshan University. His current research interests include indoor localization and wireless sensor network.

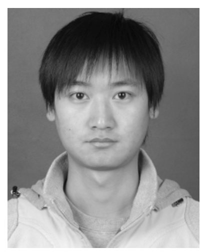

Yazhou Yuan received the B.S. and M.S. degrees in control science and engineering from Yanshan University, Qinhuangdao, China, in 2009 and 2012, respectively, and the Ph.D. degree in control theory and engineering from Shanghai Jiao Tong University in 2016. He is currently an Associate Professor with the Institute of Electrical Engineering, Yanshan University. His research interests include real-time location algorithm and the industrial Internet of Things.

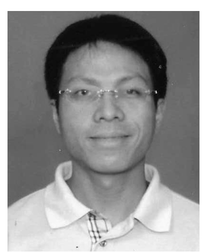

Kit Yan Chan (Member, IEEE) received the Ph.D. degree in computing from London South Bank University, London, U.K., in 2006. He is a Senior Lecturer with the Department of Electrical and Computer Engineering, Curtin University, Perth, WA, Australia. His research interests include machine learning, pattern recognition, and algorithm design.

Authorized licensed use limited to: University of Adelaide. Downloaded on September 03,2021 at 01:18:45 UTC from IEEE Xplore. Restrictions apply.